Inorg. Chem. **2007**, *46*, 533–540

Inorganic Chemistry
Article

Multiple Additions of Phenylgermanium Ligands to Tetraruthenium and Tetraosmium Carbonyl Cluster Complexes

Richard D. Adams,* Erin M. Boswell, Burjor Captain, and Mitul A. Patel

Department of Chemistry and Biochemistry, University of South Carolina, Columbia, South Carolina 29208

Received October 24, 2006

Three new compounds, $Ru_4(\mu_4\text{-}GePh)_2(\mu\text{-}GePh_2)_2(\mu\text{-}CO)_2(CO)_8$ (**11**), $Ru_4(\mu_4\text{-}GePh)_2(\mu\text{-}GePh_2)_3(\mu\text{-}CO)(CO)_8$ (**12**), and $Ru_4(\mu_4\text{-}GePh)_2(\mu\text{-}GePh_2)_4(CO)_8$ (**13**), were obtained from the reaction of $H_4Ru_4(CO)_{12}$ with excess Ph_3GeH in octane (**11** and **12**) or decane (**13**) reflux. Compound **11** was converted to compound **13** by reaction with Ph_3GeH by heating solutions in nonane solvent to reflux. Compounds **11**–**13** each contain a square-type arrangement of four Ru atoms capped on each side by a quadruply bridging GePh ligand to form an octahedral geometry for the Ru_4Ge_2 group. Compound **11** also contains two edge-bridging $GePh_2$ groups on opposite sides of the cluster and two bridging carbonyl ligands. Compound **12** contains three edge-bridging $GePh_2$ groups and one bridging carbonyl ligand. Compound **13** contains four bridging $GePh_2$ groups, one on each edge of the Ru_4 square. The reaction of $H_4Os_4(CO)_{12}$ with excess Ph_3GeH in decane at reflux yielded two new tetraosmium cluster complexes, $Os_4(\mu_4\text{-}GePh)_2(\mu\text{-}GePh_2)_3(\mu\text{-}CO)(CO)_8$ (**14**) and $Os_4(\mu_4\text{-}GePh)_2(\mu\text{-}GePh_2)_4(CO)_8$ (**15**). These compounds are structurally similar to compounds **12** and **13**, respectively.

Introduction

Tin[1] and germanium[2] are widely used as modifiers to control the reactivity and selectivity of transition-metal catalysts. Ruthenium catalysts derived from cluster complexes combined with group 14 elements, germanium, tin, and lead, have also been found to exhibit interesting catalytic properties.[3] For example, we have recently shown that the trimetallic catalyst $PtRu_5Sn$ (1−2-nm particles on a silica mesopore), obtained from the molecular precursor $PtRu_5(SnPh_2)(CO)_{15}(\mu_6\text{-}C)$, is an excellent catalyst for the selective hydrogenation of dimethyl terephthalate to cyclohexanedimethanol, a valuable linker in the polymer industry.[4]

In recent studies, we have demonstrated that triphenylstannane (Ph_3SnH) is an excellent reagent for the multiple addition of phenyltin ligands to polynuclear transition-metal carbonyl cluster complexes. For example, $Ru_5(CO)_{12}(C_6H_6)(\mu_5\text{-}C)$ reacts with Ph_3SnH to yield two compounds: $Ru_5(CO)_8(C_6H_6)(\mu\text{-}SnPh_2)_4(\mu_5\text{-}C)$ (**1**) and $Ru_5(CO)_7(C_6H_6)(\mu\text{-}SnPh_2)_4(SnPh_3)(\mu_5\text{-}C)(\mu\text{-}H)$ (**2**).[5] Ph_3SnH also reacts with $M_4(CO)_{12}$ (M = Rh, Ir) to yield bimetallic cluster complexes

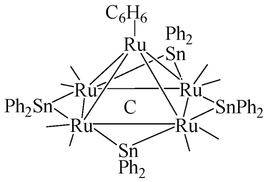

1

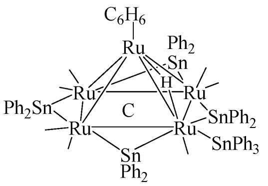

2

---

* To whom correspondence should be addressed. E-mail: adams@mail.chem.sc.edu.

[1] (a) Holt, M. S.; Wilson, W. L.; Nelson, J. H. *Chem. Rev.* **1989**, *89*, 11. (b) Coupé, J. N.; Jordão, E.; Fraga, M. A.; Mendes, M. J. *Appl. Catal. A* **2000**, *199*, 45. (c) Santos, S. M.; Silva, A. M.; Jordao, E.; Fraga, M. A. *Catal. Commun.* **2004**, *5*, 377. (d) Toba, M.; Tanaka, S.; Niwa, S.; Mizukami, F.; Koppany, Z.; Guczi, L.; Cheah, K.-Y.; Tang, T.-S. *Appl. Catal. A* **1999**, *189*, 243.

[2] (a) Lafaye, G.; Micheaud-Especel, C.; Montassier, C.; Marecot, P.; *Appl. Catal. A* **2002**, *230*, 19. (b) Didillon, B.; Candy, J. P.; Lepepetier, F.; Ferretti, O. A.; Basset, J. M. *Stud. Surf. Sci. Catal.* **1993**, *78*, 147. (c) Lafaye, G.; Mihut, C.; Especel, C.; Marecot, P.; Amiridis, M. D. *Langmuir* **2004**, *20*, 10612.

[3] (a) Hermans, S.; Raja, R.; Thomas, J. M.; Johnson, B. F. G.; Sankar, G.; Gleeson, D. *Angew. Chem., Int. Ed.* **2001**, *40*, 1211. (b) Hermans, S.; Johnson, B. F. G. *Chem. Commun.* **2000**, 1955. (c) Raja, R.; Khimyak, T.; Thomas, J. M.; Hermans, S.; Johnson, B. F. G. *Angew. Chem., Int. Ed.* **2001**, *40*, 4638. (d) Tijani, A.; Coq, B.; Figueras, F. *Appl. Catal.* **1991**, *76*, 255. (e) Sanchez-Sierra, M. C.; García-Ruiz, J.; Proietti, M. G.; Blasco, J. *J. Mol. Catal. A* **1996**, *108*, 95.

[4] Hungria, A.; Raja, R.; Adams, R. D.; Captain, B.; Thomas, J. M.; Midgley, P.; Golovko, V.; Johnson, B. F. G. *Angew. Chem., Int. Ed.* **2006**, *45*, 4782.

[5] (a) Adams, R. D.; Captain, B.; Fu, W.; Smith, M. D. *Inorg. Chem.* **2002**, *41*, 5593. (b) Adams, R. D.; Captain, B.; Fu, W.; Smith, M. D. *Inorg. Chem.* **2002**, *41*, 2302.

10.1021/ic062039w CCC: $37.00

that contain very large numbers of phenyltin ligands.[6] Some examples of these complexes include $M_3(CO)_6(SnPh_3)_3(\mu\text{-}SnPh_2)_3$ [M = Rh (**3**) and Ir (**4**)] and $Rh_3(CO)_3(SnPh_3)_3(\mu\text{-}SnPh_2)_3(\mu_3\text{-}SnPh)_2$ (**5**). The latter compound contains the first examples of triply bridging SnPh ligands.[6]

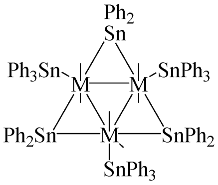

3: M = Rh
4: M = Ir

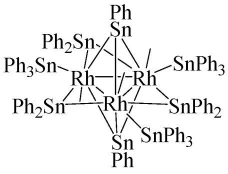

5

We have also shown that triphenylgermane, Ph_3GeH, engages in multiple addition reactions to ruthenium, iridium, and rhodium cluster complexes to yield complexes with bridging $GePh_2$ and GePh ligands. Some examples of these cluster complexes include $Ru_5(CO)_{11}(\mu\text{-}GePh_2)_4(\mu_5\text{-}C)$ (**6**),[7] $Ir_3(\mu\text{-}GePh_2)_3(GePh_3)_3(CO)_6$ (**7**),[8] $Ir_4H_4(\mu\text{-}GePh_2)_4(\mu_4\text{-}GePh)_2(CO)_4$ (**8**),[8] $Rh_8(\mu_4\text{-}GePh)_6(CO)_{12}$ (**9**),[9] and $Rh_3(GePh_3)(\mu\text{-}GePh_2)_3(\mu_3\text{-}GePh)(\mu\text{-}H)(CO)_5$ (**10**).[9] The addition of these bridging MPh_2 groups (M = Ge, Sn) occurs by the initial oxidative addition of the M−H bond to the cluster to yield MPh_3 and hydrido ligands.[5a] The formation of the MPh_2 group then occurs by cleavage of a Ph group from an intermediate containing a MPh_3 ligand. The cleaved phenyl group then combines with a hydride ligand and is eliminated as C_6H_6.[5a]

There are very few examples of ruthenium or osmium carbonyl cluster complexes containing germanium ligands reported in the literature.[10] The few that do exist contain either terminal GeR_3 groups or bridging GeR_2 groups. We have now investigated the reactions of $H_4M_4(CO)_{12}$ (M = Ru,[11] Os[12]) with Ph_3GeH, which have afforded new tetranuclear metal carbonyl cluster complexes with the general formula $M_4(\mu_4\text{-}GePh)_2(\mu\text{-}GePh_2)_{2+n}(CO)_{10-n}$ (where M = Ru, $n = 0$, 1, or 2, and where M = Os, $n = 1$ or 2) containing unusually large numbers of phenylgermanium ligands. These compounds also provide the first examples of ruthenium and osmium cluster complexes that contain quadruply bridging GePh ligands. The synthesis and structural characterization of these new compounds is presented in this report.

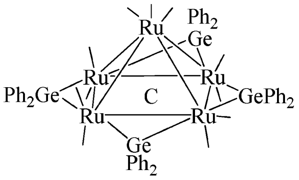

6

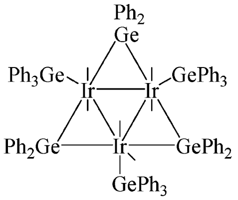

7

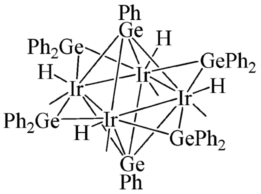

8

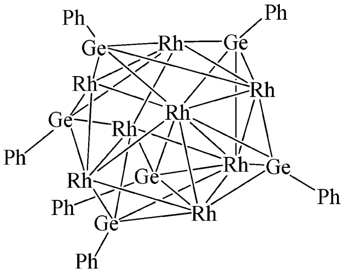

9

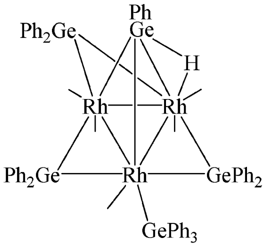

10

Results and Discussion

The reaction of $H_4Ru_4(CO)_{12}$ with an excess of Ph_3GeH in octane at reflux (125 °C) yielded two new tetraruthenium cluster complexes, $Ru_4(\mu_4\text{-}GePh)_2(\mu\text{-}GePh_2)_2(\mu\text{-}CO)_2(CO)_8$ (**11**) and $Ru_4(\mu_4\text{-}GePh)_2(\mu\text{-}GePh_2)_3(\mu\text{-}CO)(CO)_8$ (**12**), in 53% and 10% yield, respectively (see Scheme 1). Both compounds were characterized by a combination of IR, ^1H NMR, single-crystal X-ray diffraction, and mass spectral analyses. A summary of the crystal data analysis for all the compounds is given in Tables 1 and 2.

An ORTEP diagram of the molecular structure of **11** is shown in Figure 1. Selected intramolecular bond distances and angles are listed in Tables 3 and 4, respectively. The molecule contains a crystallograhically imposed center of symmetry. The molecule contains a rectangular cluster of four Ru atoms bridged by two quadruply bridging GePh ligands that cap each side of the Ru_4 rectangle. There are also two $GePh_2$ groups that bridge two opposite edges of the Ru_4 rectangle, and there are two trans-positioned edge-bridging CO ligands that lie cis to the bridging $GePh_2$ ligands. Each Ru atom contains two terminally coordinated CO ligands. Because of the crystal symmetry, there are only two independent Ru−Ru bond distances. The Ru−Ru bonds bridged by CO ligands [Ru1−Ru2* = Ru2−Ru1* = 2.8188(7) Å] are significantly shorter than the Ru−Ru bonds bridged by $GePh_2$ ligands [Ru1−Ru2 = Ru1*−Ru2* = 2.9508(9) Å]. The average value for the unbridged Ru−Ru

---

(6) Adams, R. D.; Captain, B.; Smith, J. L., Jr.; Hall, M. B.; Beddie, C. L.; Webster, C. E. *Inorg. Chem.* **2004**, *43*, 7576.
(7) Adams, R. D.; Captain, B.; Fu, W. *Inorg. Chem.* **2003**, *42*, 1328.
(8) Adams, R. D.; Captain, B.; Smith, J. L., Jr. *Inorg. Chem.* **2005**, *44*, 1413.
(9) Adams, R. D.; Smith, J. L., Jr. *Inorg. Chem.* **2005**, *44*, 4276.
(10) (a) Pomeroy, R.; Einstein, F. W. B.; Leong, W. K. *Organometallics* **1996**, *15*, 1589. (b) Baya, M.; Esteruelas, M. A.; Onate, E. *Organometallics* **2001**, *20*, 4875. (c) Baya, M.; Crochet, P.; Esteruelas, M. A.; Onate, E. *Organometallics* **2001**, *20*, 240. (d) Jiang, F.; Biradha, K.; Leong, W. K.; Pomeroy, R. K.; Zaworotko, M. J. *Can. J. Chem.* **1999**, *77*, 1327. (e) Clark, G. R.; Flower, K. R.; Rickard, C. E. F.; Roper, W. R.; Salter, D. M.; Wright, L. J. *J. Organomet. Chem.* **1993**, *462*, 331.
(11) Kaesz, H. D.; Knox, S. A. R.; Koepke, J. W.; Andrews, M. A. *J. Am. Chem. Soc.* **1975**, *97*, 3942.
(12) Zuccaro, C. *Inorg. Synth.* **1989**, *26*, 293.

Scheme 1

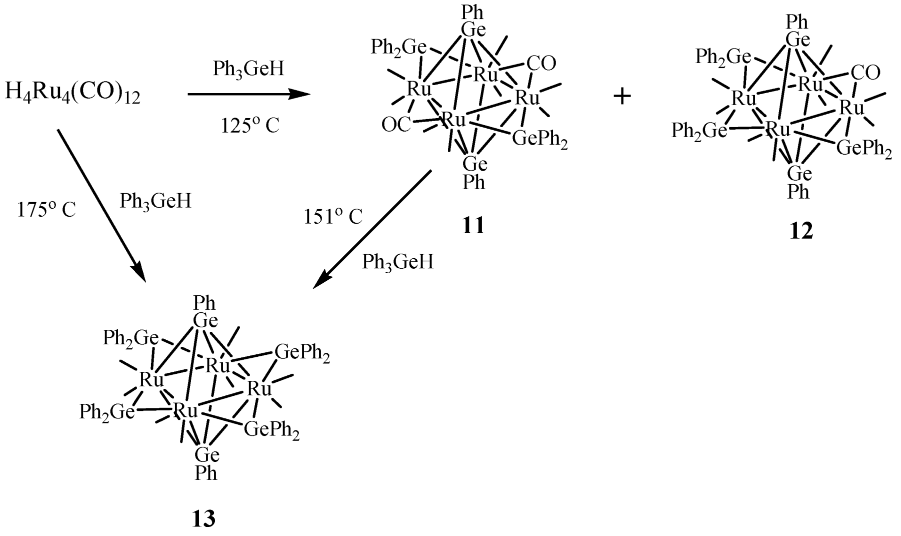

bond distances in $Ru_3(CO)_{12}$ is 2.854(1) Å.[13] The Ru−Ru distance in the triruthenium compound $Ru_3(\mu\text{-}GeMe_2)_3(CO)_9$, which has three edge-bridging $GeMe_2$ ligands, is 2.926(9) Å.[14] Compound **11** appears to be the first example of a ruthenium complex to contain quadruply bridging GeR ligands. The Ru−Ge distances to the quadruply bridging GePh ligands are slightly longer, 2.5857(9), 2.5497(10), 2.5565(10), and 2.5580(8) Å, than the Ru−Ge distances to the edge-bridging $GePh_2$ ligands, 2.4871(9) and 2.4910(9) Å. This can be attributed to the higher coordination (five) of the quadruply bridging GePh ligands compared to the lower coordination (four) of the edge-bridging $GePh_2$ ligands. For comparison, the Ru−Ge distances in $Ru_3(\mu\text{-}GeMe_2)_3(CO)_9$ are 2.482(11)−2.500(12) Å.[14] Other examples of metal cluster complexes that contain quadruply bridging GeR ligands include $Co_4(CO)_{11}(\mu_4\text{-}GeMe)_2$,[15] $Ni_9(CO)_8(\mu_4\text{-}GeEt)_6$,[16] and $Ir_4(\mu\text{-}GePh_2)_4(\mu_4\text{-}GePh)_2H_4(CO)_4$.[7] The bridging $GePh_2$ groups in **11** are displaced slightly out of the Ru_4 least-squares plane, one above and one below by ±0.167 Å. The bridging CO ligands are also displaced slightly out of the Ru_4 plane (±0.092 Å) on opposite sides.

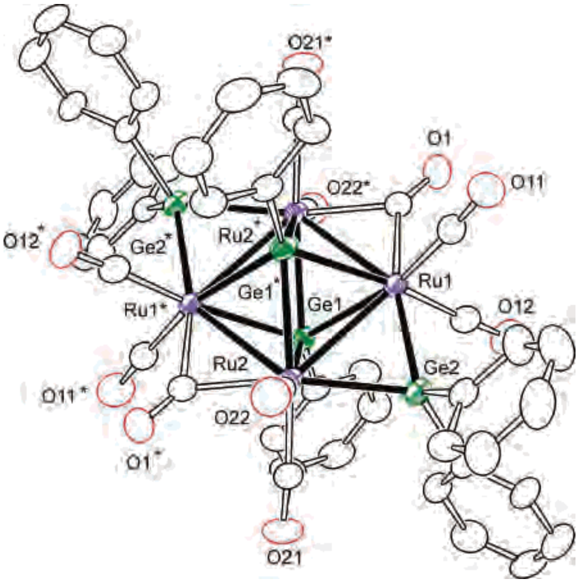

Figure 1. ORTEP diagram of **11** showing 30% thermal ellipsoid probability.

An ORTEP diagram of **12** is shown in Figure 2. Selected intramolecular bond distances and angles are listed in Tables 3 and 4. The structure of compound **12** is similar to that of **11** except in place of a bridging CO group there is a bridging $GePh_2$ group. The four Ru atoms in **12** have a trapezoidal-like arrangement of four Ru atoms. There are two quadruply bridging GePh ligands, three edge-bridging $GePh_2$ ligands, and one bridging CO ligand. Each Ru atom has two terminal CO ligands. The Ru−Ru bond that is bridged by the CO ligand, Ru3−Ru4 = 2.8103(6) Å, is significantly shorter than the three Ru−Ru bonds that are bridged by $GePh_2$ ligands, Ru1−Ru2 = 2.9638(6) Å, Ru1−Ru4 = 2.9313(6) Å, and Ru2−Ru3 = 2.9399(6) Å. The Ru−Ru and Ru−Ge distances in **12** are similar to the corresponding bond distances in **11**. The bridging $GePh_2$ ligands are displaced out of the Ru_4 least-squares plane, two on one side, Ge3 by −0.335 Å and Ge5 by −0.351 Å, while the third bridging $GePh_2$ group, Ge4, is displaced on the opposite side of the Ru_4 square plane by 0.438 Å. The bridging CO ligand is displaced out of the Ru_4 plane by 0.143 Å on the same side as Ge4.

At 175 °C, the reaction of $H_4Ru_4(CO)_{12}$ with excess Ph_3GeH yielded the new compound $Ru_4(\mu_4\text{-}GePh)_2(\mu\text{-}GePh_2)_4(CO)_8$ (**13**) in a 76% yield. Compound **13** was also characterized by a combination of IR, ^1H NMR, single-crystal X-ray diffraction, and mass spectral analyses. An ORTEP diagram of the molecular structure of **13** is shown in Figure 3. Selected intramolecular bond distances and angles are given in Tables 3 and 4. The molecule contains an approximately square arrangement of four Ru atoms with two quadruply bridging GePh ligands and a bridging $GePh_2$ on each edge of the Ru_4 square. Each Ru atom has two CO ligands that are terminally coordinated. Compound **13**

---

(13) Churchill, M. R.; Hollander, F. J.; Hutchinson, J. P. *Inorg. Chem.* **1977**, *16*, 2655.

(14) Howard, J.; Woodward, P. *J. Chem. Soc. A* **1971**, 3648.

(15) Foster, S. P.; Mackay, K. M.; Nicholson, B. K. *Chem. Commun.* **1982**, 1156.

(16) Zebrowski, J. P.; Hayashi, R. K.; Bjarnason, A.; Dahl, L. F. *J. Am. Chem. Soc.* **1992**, *114*, 3121.

Table 1. Crystallographic Data for Compounds **11**−**13**

	11	**12**	**13**
empirical formula	$Ru_4Ge_4O_{10}C_{46}H_{30}$	$Ru_4Ge_5O_9C_{57}H_{40}$	$Ru_4Ge_6O_8C_{68}H_{50}\cdot 2\ C_4H_{10}O$
fw	1437.34	1636.12	1983.14
cryst syst	monoclinic	orthorhombic	orthorhombic
lattice parameters			
a (Å)	9.5604(6)	12.8681(5)	11.7557(7)
b (Å)	23.3208(14)	21.9498(9)	25.4240(16)
c (Å)	11.4639(7)	23.1450(10)	24.7493(16)
α (deg)	90	90	90
β (deg)	112.570(1)	90	90
γ (deg)	90	90	90
V (Å^3)	2360.2(3)	6537.5(5)	7397.0(8)
space group	$P2_1/c$ (No. 14)	$P2_12_12_1$ (No. 19)	$C222_1$ (No. 20)
Z value	2	4	4
ρ_{calc} (g/cm^3)	2.023	1.662	1.781
μ(Mo Kα) (mm^{-1})	3.809	3.208	3.249
T (K)	294	294	100
$2\theta_{max}$ (deg)	50.06	56.70	56.62
no. obsd reflns [$I > 2\sigma(I)$]	2892	13 862	8513
no. of param	289	676	438
GOF	1.031	1.106	1.025
max shift in cycle	0.000	0.001	0.002
residuals:[a] R1; wR2	0.0367; 0.0808	0.0352; 0.1002	0.0258; 0.0579
abs corrn, max/min	multiscan, 1.000/0.681	multiscan, 1.000/0.832	multiscan, 1.000/0.822
largest peak in the final diff map (e/Å^3)	1.578	1.266	1.743

[a] $R1 = \Sigma_{hkl}(||F_o| - |F_c||)/\Sigma_{hkl}|F_o|$; $wR2 = [\Sigma_{hkl}w(|F_o| - |F_c|)^2/\Sigma_{hkl}wF_o^2]^{1/2}$, $w = 1/\sigma^2(F_o)$; $GOF = [\Sigma_{hkl}w(|F_o| - |F_c|)^2/(n_{data} - n_{vari})]^{1/2}$.

Table 2. Crystallographic Data for Compounds **14** and **15**

	14	**15**
empirical formula	$Os_4Ge_5O_9C_{57}H_{40}\cdot C_7H_8$	$Os_4Ge_6O_8C_{68}H_{50}\cdot {}^1/_4C_4H_{10}O$
fw	2084.77	2209.95
cryst syst	triclinic	monoclinic
lattice parameters		
a (Å)	14.1902(6)	15.7900(6)
b (Å)	17.1633(7)	17.9143(7)
c (Å)	18.0443(7)	25.297(1)
α (deg)	104.846(1)	90
β (deg)	106.665(1)	91.869(1)
γ (deg)	112.665(1)	90
V (Å^3)	3534.9(2)	7151.8(5)
space group	$P\bar{1}$ (No. 2)	$P2_1/c$ (No. 14)
Z value	2	4
ρ_{calc} (g/cm^3)	1.959	2.052
μ(Mo Kα) (mm^{-1})	9.299	9.607
T (K)	150	294
$2\theta_{max}$ (deg)	56.62	56.64
no. of obsd reflns [$I > 2\sigma(I)$]	15 301	13 934
no. of param	740	795
GOF	1.059	1.114
max shift in cycle	0.002	0.002
residuals;[a] R1; wR2	0.0288; 0.0939	0.0309; 0.0855
abs corrn, max/min	multiscan, 1.000/0.438	multiscan, 1.000/0.569
largest peak in the final diff map (e/Å^3)	2.870	2.457

[a] $R1 = \Sigma_{hkl}(||F_o| - |F_c||)/\Sigma_{hkl}|F_o|$; $wR2 = [\Sigma_{hkl}w(|F_o| - |F_c|)^2/\Sigma_{hkl}wF_o^2]^{1/2}$, $w = 1/\sigma^2(F_o)$; $GOF = [\Sigma_{hkl}w(|F_o| - |F_c|)^2/(n_{data} - n_{vari})]^{1/2}$.

contains a crystallographically imposed 2-fold rotational axis that passes through the two atoms Ge1 and Ge2. All four Ru−Ru bond distances are very similar and similar to the $GePh_2$ bridged distances in **11** and **12**. The two independent Ru−Ru distances are Ru1−Ru2 = 2.9428(3) Å and Ru1−Ru2* = 2.9249(3) Å. The Ru−Ru and Ru−Ge distances in **13** are similar to the corresponding bond distances in **11** and **12**. The $GePh_2$ ligands in **13** are displaced out of the Ru_4 plane slightly farther than the $GePh_2$ ligands in **11** and **12**. Ge3 and Ge3* lie −0.443 Å out of the Ru_4 plane, and Ge4 and Ge4* are displaced by 0.302 Å to the opposite side of the plane. This is probably due to increased steric interactions between the four $GePh_2$ ligands and the CO ligands.

The reaction of Ph_3GeH with $H_4Os_4(CO)_{12}$ was also investigated. Relatively high temperatures were required to initiate a reaction, but at 175 °C, two new compounds, $Os_4(\mu_4\text{-}GePh)_2(\mu\text{-}GePh_2)_3(\mu\text{-}CO)(CO)_8$ (**14**) in 28% yield and $Os_4(\mu_4\text{-}GePh)_2(\mu\text{-}GePh_2)_4(CO)_8$ (**15**) in 2% yield, were obtained (see Scheme 2). Interestingly, we found no evidence for an Os_4Ge_4 compound analogous to **11** under these conditions, and at lower temperatures, there was no significant reaction at all. Compounds **14** and **15** were characterized by a combination of IR, ^1H NMR, single-crystal X-ray diffraction, and mass spectral analyses. Compounds **14** and **15** are similar to **12** and **13** described above.

An ORTEP diagram of **14** is shown in Figure 4. Selected intramolecular bond distances and angles are listed in Tables 5 and 6, respectively. Compound **14** consists of a trapezoidal arrangement of four Os atoms with three bridging $GePh_2$ and one bridging CO. There are also two quadruply bridging GePh ligands. Also, as found in each of the ruthenium compounds, each Os atom contains two terminally coordinated CO ligands. The Os−Os bond that is bridged by the CO is significantly shorter, Os3−Os4 = 2.8269(3) Å, than the Os−Os bonds that are bridged by $GePh_2$ ligands, Os1−Os2 = 2.9540(3) Å, Os1−Os4 = 2.9318(3) Å, and Os2−Os3 = 2.9261(3) Å. This finding is consistent with the structure of the ruthenium analogue **12**. The average value for the unbridged Os−Os bond distances in $Os_3(CO)_{12}$ is 2.877(3) Å.[17] The Os−Os bond distance in the triosmium compound $Os_3(CO)_9(\mu\text{-}GeMe_2)_3$, which has three edge-bridging $GeMe_2$ ligands, is 2.920(1) Å.[10a] As was found for the ruthenium analogues **12** and **13**, the $GePh_2$ groups are

---

(17) Churchill, M. R.; DeBoer, B. G. *Inorg. Chem.* **1977**, *16*, 878.

Table 3. Selected Intramolecular Bond Distances for Compounds **11**−**13**[a]

11			12			13		
atom	atom	distance (Å)	atom	atom	distance (Å)	atom	atom	distance (Å)
Ru1	Ru2	2.9508(9)	Ru1	Ru2	2.9638(6)	Ru1	Ru2	2.9428(3)
Ru1	Ru2*	2.8188(7)	Ru1	Ru4	2.9313(6)	Ru1	Ru2*	2.9249(3)
Ru1	Ge1	2.5857(9)	Ru2	Ru3	2.9399(6)	Ru1	Ge3	2.4776(4)
Ru1*	Ge1	2.5497(10)	Ru3	Ru4	2.8103(6)	Ru1	Ge4	2.4817(4)
Ru2	Ge1	2.5565(10)	Ru1	Ge1	2.5497(7)	Ru2	Ge3*	2.4866(4)
Ru2*	Ge1	2.5580(8)	Ru2	Ge1	2.5643(7)	Ru2	Ge4	2.4891(4)
Ru1	Ge2	2.4871(9)	Ru3	Ge1	2.5686(7)	Ru1	Ge1	2.5648(4)
Ru2	Ge2	2.4910(9)	Ru4	Ge1	2.5709(7)	Ru2	Ge1	2.5545(4)
Ru1	C1	2.087(8)	Ru1	Ge2	2.5650(7)	Ru1	Ge2	2.5815(4)
Ru2	C1*	2.093(8)	Ru2	Ge2	2.5323(7)	Ru2	Ge2	2.5886(4)
C	O	1.141(6) av	Ru3	Ge2	2.6076(7)	C	O	1.139(6)
			Ru4	Ge2	2.5524(7)			
			Ru1	Ge3	2.5013(7)			
			Ru1	Ge4	2.5045(7)			
			Ru2	Ge4	2.4841(7)			
			Ru2	Ge5	2.4897(7)			
			Ru3	Ge5	2.4847(7)			
			Ru4	Ge3	2.4988(7)			
			Ru3	C1	2.118(7)			
			Ru4	C1	2.052(6)			
			C	O	1.135(6) av			

[a] Estimated standard deviations in the least significant figure are given in parentheses. Asterisks indicate atoms generated by symmetry.

Table 4. Selected Intramolecular Bond Angles for Compounds **11**−**13**[a]

11				12				13			
atom	atom	atom	angle (deg)	atom	atom	atom	angle (deg)	atom	atom	atom	angle (deg)
Ru1	Ru2	Ru1*	90.37(3)	Ru1	Ru2	Ru3	89.01(6)	Ru1	Ru2	Ru1*	90.055(9)
Ru2	Ru1*	Ru2*	89.63(3)	Ru1	Ru4	Ru3	92.21(7)	Ru2	Ru1*	Ru2*	89.941(9)
Ru1	C1	Ru2*	84.80(4)	Ru2	Ru3	Ru4	90.76(7)	Ru1	Ge3	Ru2*	72.20(1)
Ru1	Ge2	Ru2	72.70(6)	Ru2	Ru1	Ru4	87.97(6)	Ru1	Ge4	Ru2	72.60(1)
Ru1	Ge1	Ru2*	66.46(6)	Ru1	Ge3	Ru4	71.78(2)	Ru1	Ge1	Ru2	70.18(1)
Ru1	Ge1	Ru2	70.03(4)	Ru1	Ge4	Ru2	72.90(2)	Ru1	Ge1	Ru2*	69.69(1)
Ru1*	Ge1	Ru2	67.01(7)	Ru2	Ge5	Ru3	72.46(2)	Ru1	Ge2	Ru2	69.39(1)
Ru1*	Ge1	Ru2*	70.58(5)	Ru3	C1	Ru4	84.70(2)	Ru1	Ge2	Ru2*	68.90(1)
Ru1	Ge1	Ru1*	105.73(3)	Ru1	Ge1	Ru2	70.84(9)	Ru1	Ge1	Ru1*	108.04(2)
Ru2*	Ge1*	Ru2	105.37(5)	Ru1	Ge1	Ru4	69.84(2)	Ru2	Ge1	Ru2*	108.52(2)
				Ru2	Ge1	Ru3	69.89(2)	Ru1	Ge2	Ru1*	107.03(2)
				Ru3	Ge1	Ru4	66.30(2)	Ru2	Ge2	Ru2*	106.45(2)
				Ru1	Ge2	Ru2	71.10(2)				
				Ru1	Ge2	Ru4	69.89(2)				
				Ru2	Ge2	Ru3	69.76(9)				
				Ru3	Ge2	Ru4	65.99(9)				
				Ru1	Ge1	Ru3	107.91(2)				
				Ru2	Ge1	Ru4	105.73(2)				
				Ru1	Ge2	Ru3	106.27(2)				
				Ru2	Ge2	Ru4	107.25(2)				

[a] Estimated standard deviations in the least significant figure are given in parentheses. Asterisks indicate atoms generated by symmetry.

displaced out of the plane of the four Os atoms. The Ge atoms, Ge3 and Ge5, for the two bridging $GePh_2$ ligands positioned trans to each other are displaced to one side of the Os_4 square plane by −0.450 and −0.398 Å, respectively, while the other bridging $GePh_2$ group, Ge4, is displaced to the other side of the plane by 0.507 Å. The C atom of the bridging CO ligand, C1, is displaced out of the Os_4 square plane to the same side as Ge4 by 0.363 Å. From a crystallographic viewpoint, it is worth noting that compounds **12** and **14** are isostructural but are not isomorphous. This is because a toluene solvent molecule cocrystallized with **14**, while in **12**, no solvent was cocrystallized with the compound.

An ORTEP diagram of **15** is shown in Figure 5. Selected intramolecular bond distances and angles are listed in Tables 5 and 6, respectively. Compound **15** contains four Os atoms in approximately a square arrangement. As in **13**, there are two quadruply bridging GePh ligands and four bridging $GePh_2$. Each Os atom contains two terminal CO ligands. All four Os−Os bond lengths in **15** are similar to each other and also similar to the $GePh_2$ bridged bonds in **14**: Os1−Os2 = 2.9280(3) Å, Os1−Os4 = 2.9283(3) Å, Os2−Os3 = 2.9609(3) Å, and Os3−Os4 = 2.9346(3) Å. Like **14**, the $GePh_2$ ligands are displaced out of the Os_4 least-squares plane. The atoms Ge3 and Ge5 are displaced to one side of the plane by −0.414 and −0.499 Å, respectively, while Ge4 and Ge6 are both displaced to the other side of the Os_4 plane by 0.350 and 0.421 Å, respectively. Just like the analogous compounds **12** and **14**, compounds **13** and **15** are also isostructural but are not isomorphous. This is because both compounds cocrystallized with the solvent of crystallization

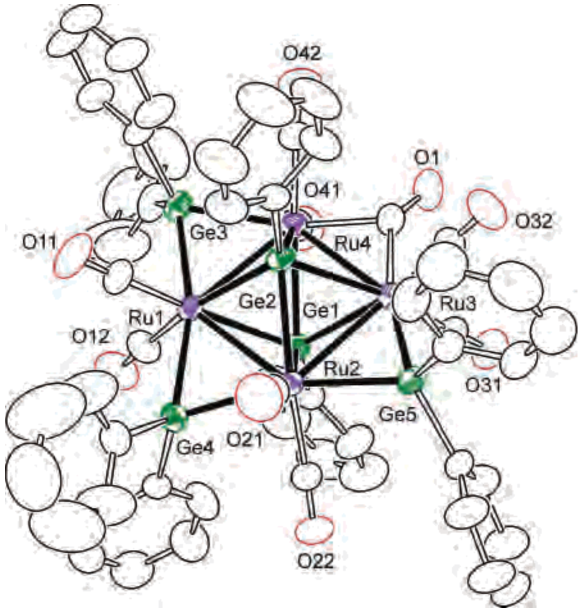

Figure 2. ORTEP diagram of **12** showing 30% thermal ellipsoid probability.

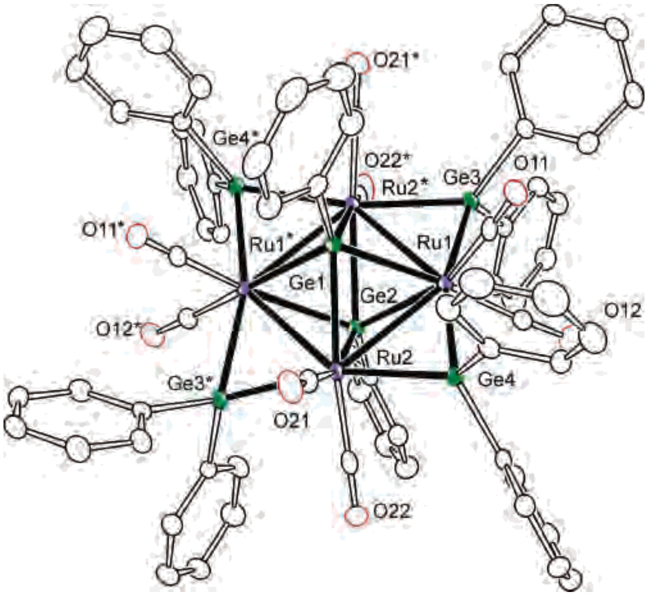

Figure 3. ORTEP diagram of **13** showing 50% thermal ellipsoid probability.

(diethyl ether); however, the number of solvent molecules present in the crystal lattice for these two compounds was different.

Each of the new compounds reported here, **11**−**15**, contains four metal atoms and has a total of 62 cluster valence electrons. This is in accord with the Polyhedral Skeletal Electron Pair theory, which predicts $14n + 6$ electrons for *arachno*-octahedra,[18] $n = 4$, but differs from the 18-electron rule, which predicts 64 electrons, $18n - 2m$, $m =$ the number of metal−metal bonds. There are many examples of square M_4 cluster complexes containing two quadruply bridging ligands on each side of the M_4 cluster.[19] Many of these have 62 cluster valence electrons. There are some that have 64 cluster valence electrons, but the number with 62 valence electrons is by far the greater of the two types.

During the course of the formation of compounds **11**−**15**, the core of the tetrahedral M_4 clusters of the starting compounds $H_4M_4(CO)_{12}$ (M = Ru, Os) is opened and transformed into the square-type arrangement. Transformations such as this have been observed on previous occasions.[19] The process involves cleavage of a minimum of two metal−metal bonds and can proceed stepwise through the formation of a butterfly tetrahedral intermediate. The transformation is shown schematically in Scheme 3. These bond cleavages are usually induced by the addition of electrons to the complexes upon the addition of ligands to the metal atoms. Indeed, the $H_4M_4(CO)_{12}$ clusters have only 60 valence electrons, and our final products have 62. Although there are a number of examples of transformations such as those shown in Scheme 3,[20−22] in this work, we did not observe any products having butterfly tetrahedral M_4 clusters. We have already reported a similar transformation of the tetrahedral cluster complex $Ir_4(CO)_{12}$ into the Ir_4 square planar cluster **8** upon reaction with Ph_3GeH at 151 °C.[8]

The formation of the $GePh_2$ and GePh ligands in the course of these reactions is presumed to occur by cleavage of the Ph groups from Ph_3GeH and its combination with hydride ligands to eliminate benzene. This is based on our previous finding for reactions of Ph_3SnH with other metal carbonyl cluster complexes.[5a]

Experimental Section

General Data. All reactions were performed under a N_2 atmosphere using standard Schlenk techniques. Reagent-grade solvents were dried by standard procedures and were freshly distilled prior to their use. IR spectra were recorded on a Nicolet Avatar 360 Fourier transform IR spectrophotometer. ^1H NMR spectra were recorded on a Varian Mercury 400 spectrometer operating at 400 MHz. Mass spectrometric (MS) measurements performed by a direct-exposure probe using electron impact ionization (EI) were made on a VG 70S instrument. Triphenylgermanium hydride, Ph_3GeH, was purchased from Aldrich and was used without further purification. Nonane (99%) and decane (99+%) were purchased from Alfa Aesar and were used without further purification. $H_4Ru_4(CO)_{12}$[11] and $H_4Os_4(CO)_{12}$[12] were prepared via literature methods. Product separations were performed by thin-layer chromatography (TLC) in air by using Analtech 0.25-, 0.5-, and 1.0-mm silica gel 60-Å F_{254} glass plates. Silica gel was obtained from McTony and used as received.

Reaction of $H_4Ru_4(CO)_{12}$ with Ph_3GeH at 125 °C. A 61-mg (0.200-mmol) amount of Ph_3GeH was added to a solution of 25 mg (0.033 mmol) of $H_4Ru_4(CO)_{12}$ in 20 mL of distilled octane. The reaction mixture was heated to reflux for 2 h, after which the solvent was then removed in vacuo. The residue was extracted with methylene chloride and separated by TLC over silica gel using a 3:1 (v/v) hexane/methylene chloride solvent mixture to yield in

---

(18) Mingos, D. M. P. *Acc. Chem. Res.* **1984**, *17*, 311.

(19) Thimmappa, B. H. S. *J. Cluster Sci.* **1996**, *7*, 1.

(20) Watson, W. H.; Poola, B.; Richmond, M. G. *Organometallics* **2005**, *24*, 4687.

(21) Wang, W.; Corrigan, J. F.; Enright, G.; Taylor, N. J.; Carty, A. J. *Organometallics* **1998**, *17*, 427.

(22) (a) Adams, R. D.; Wang, S. *Organometallics* **1985**, *4*, 1902. (b) Adams, R. D.; Wang, S. *Organometallics* **1986**, *5*, 1272.

Scheme 2

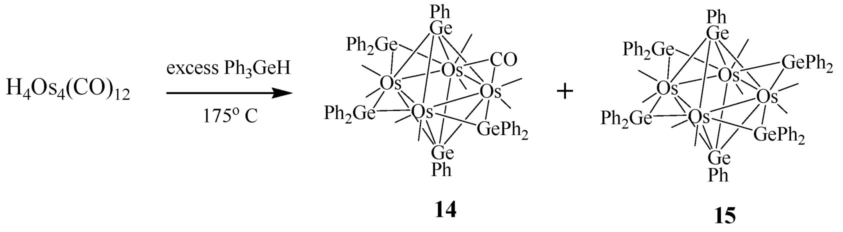

Table 5. Selected Intramolecular Bond Distances for Compounds **14** and **15**[a]

14			15		
atom	atom	distance (Å)	atom	atom	distance (Å)
Os1	Os2	2.9540(3)	Os1	Os2	2.9280(3)
Os1	Os4	2.9318(3)	Os1	Os4	2.9483(3)
Os2	Os3	2.9261(3)	Os2	Os3	2.9609(3)
Os3	Os4	2.8269(3)	Os3	Os4	2.9346(3)
Os1	Ge1	2.5560(5)	Os1	Ge1	2.5844(6)
Os2	Ge1	2.5684(5)	Os2	Ge1	2.5812(6)
Os3	Ge1	2.5939(5)	Os3	Ge1	2.5996(6)
Os4	Ge1	2.6054(5)	Os4	Ge1	2.5703(6)
Os1	Ge2	2.5807(5)	Os1	Ge2	2.5959(6)
Os2	Ge2	2.5636(5)	Os2	Ge2	2.5872(6)
Os3	Ge2	2.5878(5)	Os3	Ge2	2.5968(6)
Os4	Ge2	2.5830(5)	Os4	Ge2	2.5955(6)
Os1	Ge4	2.5108(5)	Os1	Ge3	2.5230(7)
Os1	Ge5	2.4996(5)	Os1	Ge6	2.5049(7)
Os2	Ge3	2.5186(5)	Os2	Ge3	2.5087(6)
Os2	Ge4	2.5007(5)	Os2	Ge4	2.4946(6)
Os3	Ge3	2.5132(5)	Os3	Ge4	2.4990(7)
Os4	Ge5	2.5354(5)	Os3	Ge5	2.5088(7)
Os3	C1	2.109(5)	Os4	Ge5	2.5033(6)
Os4	C1	2.105(5)	Os4	Ge6	2.5091(6)
C	O	1.140(6) av	C	O	1.137(6) av

[a] Estimated standard deviations in the least significant figure are given in parentheses.

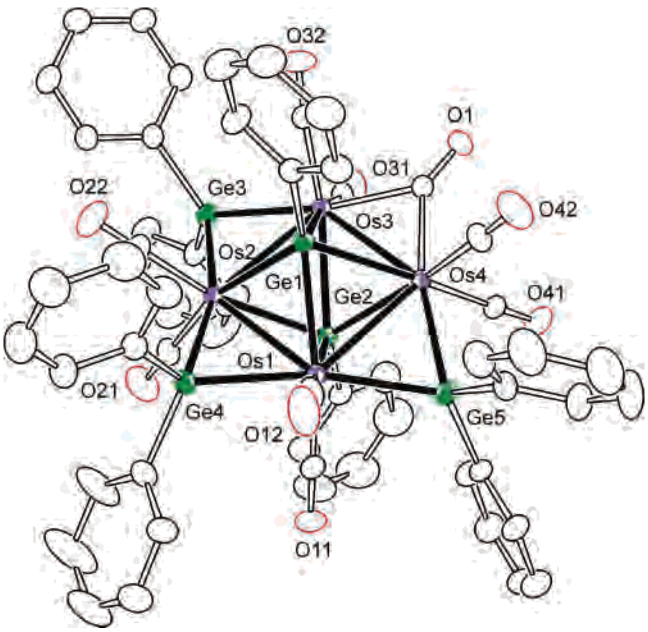

Figure 4. ORTEP diagram of **14** showing 50% thermal ellipsoid probability.

order of elution 25.9 mg (53%) of purple **11** and 5.5 mg (10%) of purple **12**. Spectral data for **11**: IR ν_{CO} (cm^{-1} in CH_2Cl_2) 2065(m), 2036(vs), 2016(sh, m), 2001(s), 1858(m, sh), 1839(m, br); ^{1}H NMR (CD_2Cl_2 in ppm) δ 6.88−6.92 (m, 5H, Ph), 7.18−7.35 (m, 20H, Ph), 7.50−7.54 (m, 5H, Ph); EI/MS *m*/*z* 1436. The isotope pattern is consistent with the presence of four Ru and four Ge atoms. Spectral data for **12**: IR ν_{CO} (cm^{-1} in CH_2Cl_2) 2050(m), 2028(s, sh), 2021(vs), 1995(s), 1977(m), 1838(w). ^{1}H NMR (C_6D_6 in ppm) δ 6.82−6.86 (m, 8H, Ph), 6.98−7.04 (m, 20H, Ph), 7.62−7.65 (m, 8H, Ph), 7.70−7.73 (m, 4H, Ph); EI/MS *m*/*z* 1637. The isotope pattern is consistent with the presence of four Ru and five Ge atoms.

Table 6. Selected Intramolecular Bond Angles for Compounds **14** and **15**[a]

14				15			
atom	atom	atom	angle (deg)	atom	atom	atom	angle (deg)
Os1	Os4	Os3	91.164(8)	Os1	Os2	Os3	90.304(9)
Os1	Os2	Os3	88.792(7)	Os1	Os4	Os3	90.422(9)
Os2	Os3	Os4	91.316(7)	Os2	Os3	Os4	89.450(8)
Os2	Os1	Os4	88.718(7)	Os2	Os1	Os4	89.822(8)
Os1	Ge4	Os2	72.233(8)	Os1	Ge3	Os2	71.17(7)
Os1	Ge5	Os4	71.38(4)	Os1	Ge6	Os4	72.03(8)
Os2	Ge3	Os3	71.12(4)	Os2	Ge4	Os3	72.73(8)
Os3	C1	Os4	84.27(8)	Os3	Ge5	Os4	71.68(7)
Os1	Ge1	Os4	69.22(3)	Os1	Ge1	Os2	69.06(6)
Os1	Ge1	Os2	70.40(4)	Os1	Ge1	Os4	69.78(6)
Os2	Ge1	Os3	69.22(3)	Os2	Ge1	Os3	69.71(6)
Os3	Ge1	Os4	65.87(3)	Os3	Ge1	Os4	69.17(5)
Os1	Ge2	Os4	69.19(3)	Os1	Ge2	Os2	68.79(6)
Os1	Ge2	Os2	70.09(4)	Os1	Ge2	Os4	69.21(6)
Os2	Ge2	Os3	69.33(3)	Os2	Ge2	Os3	69.66(6)
Os3	Ge2	Os4	66.28(3)	Os3	Ge2	Os4	68.83(6)
Os1	Ge1	Os3	106.03(8)	Os1	Ge1	Os3	107.30(2)
Os2	Ge1	Os4	105.38(8)	Os2	Ge1	Os4	107.29(2)
Os1	Ge2	Os3	105.49(8)	Os1	Ge2	Os3	107.04(2)
Os2	Ge2	Os4	106.18(8)	Os2	Ge2	Os4	106.35(2)

[a] Estimated standard deviations in the least significant figure are given in parentheses.

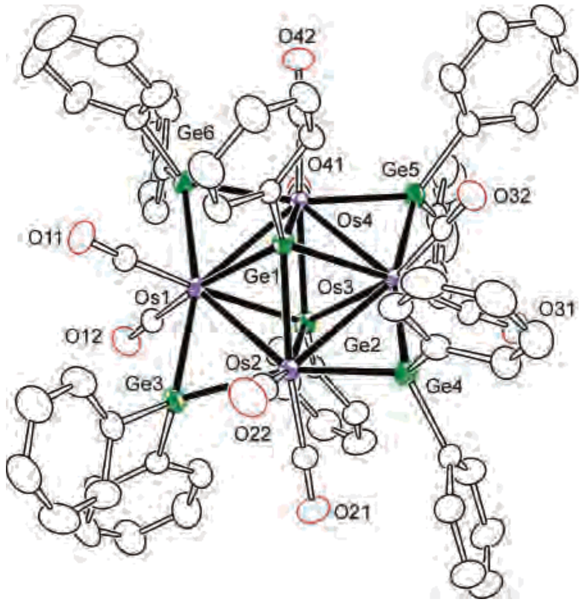

Figure 5. ORTEP diagram of **15** showing 30% thermal ellipsoid probability.

Scheme 3

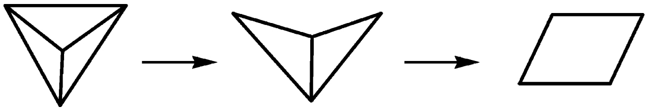

Reaction of $H_4Ru_4(CO)_{12}$ with Ph_3GeH at 175 °C. A total of 92 mg (0.302 mmol) of Ph_3GeH was added to a suspension of 15 mg (0.020 mmol) of $H_4Ru_4(CO)_{12}$ in 15 mL of decane. The mixture was heated to reflux overnight. The solvent was then removed in vacuo, and the residue was extracted with methylene chloride and run through a short column of silica gel, eluting with methylene chloride to yield 28.2 mg (76%) of blue **13**. Spectral data for **13**: IR ν_{CO} (cm^{-1} in CH_2Cl_2) 2016(vs), 1980(s); ^1H NMR (C_6D_6 in ppm) δ 6.79−6.84 (m, 8H, Ph), 6.98−7.04 (m, 24H, Ph), 7.70−7.74 (m, 18H, Ph); EI/MS *m*/*z* 1836. The isotope pattern is consistent with the presence of four Ru and six Ge atoms.

Conversion of 11 to 13. A total of 32.0 mg (0.105 mmol) of Ph_3GeH and 15.0 mg (0.010 mmol) of **11** were dissolved in 15 mL of nonane, and the solution was heated to reflux overnight. The solvent was then removed in vacuo. The residue was extracted with methylene chloride and run through a short column of silica gel, eluting with methylene chloride to yield 11.2 mg (58%) of blue **13**.

Reaction of $H_4Os_4(CO)_{12}$ with Ph_3GeH. A 27.5-mg (0.090-mmol) amount of Ph_3GeH was added to a suspension of 20 mg (0.018 mmol) of $H_4Os_4(CO)_{12}$ in 15 mL of decane. The reaction mixture was heated to reflux for 2 h. After cooling, the solvent was removed in vacuo. The residue was extracted with methylene chloride and separated by TLC over silica gel by using a 3:1 (v/v) hexane/methylene chloride solvent mixture to yield in order of elution 10.3 mg (28%) of red **14** and 1.1 mg (2%) of purple **15**. Spectral data for **14**: IR ν_{CO} (cm^{-1} in CH_2Cl_2) 2085(m), 2066(m), 2047(s), 2018(vs), 2007(s, sh), 1989(s), 1971(m), 1810(w); ^1H NMR (C_6D_6 in ppm) δ 6.68−6.72 (m, 3H, Ph), 7.16−7.32 (m, 18H, Ph), 7.42−7.51 (m, 9H, Ph), 7.52−7.57 (m, 6H, Ph), 7.67−7.72 (m, 4H, Ph); EI/MS *m*/*z* 1992. The isotope pattern is consistent with the presence of four Os and five Ge atoms. Spectral data for **15**: IR ν_{CO} (cm^{-1} in CH_2Cl_2) 2011(vs), 1973(s); ^1H NMR (C_6D_6 in ppm) δ 6.70−7.04 (m, 40H, Ph), 7.63−7.68 (m, 10H, Ph); EI/MS *m*/*z* 2192. The isotope pattern is consistent with the presence of four Os and six Ge atoms.

Crystallographic Analyses. Dark single crystals of **11** suitable for X-ray diffraction analyses were obtained by slow evaporation of the solvent at room temperature from a solution in an octane/methylene chloride solvent mixture. Dark single crystals of **12** were obtained by slow evaporation of the solvent at −25 °C from a solution in an octane/toluene solvent mixture. Dark crystals of **13** were grown from slow evaporation of the solvent from a solution in diethyl ether at −25 °C. Red crystals of **14** were obtained by slow evaporation of the solvent from a solution in an octane/toluene solvent mixture at −25 °C. Red crystals of **15** were grown by slow evaporation of the solvent from a solution in a diethyl ether solvent at −25 °C. Each data crystal was glued onto the end of a thin glass fiber. X-ray intensity data were measured by using a Bruker SMART APEX CCD-based diffractometer using Mo Kα radiation (λ = 0.710 73 Å). The raw data frames were integrated with the *SAINT+* program by using a narrow-frame integration algorithm.[23] Correction for Lorentz and polarization effects was also applied with *SAINT+*. An empirical absorption correction based on the multiple measurement of equivalent reflections was applied using the program *SADABS*. All structures were solved by a combination of direct methods and difference Fourier syntheses and refined by full-matrix least squares on F^2, using the *SHELXTL* software package.[24] All non-H atoms were refined with anisotropic displacement parameters. H atoms were placed in geometrically idealized positions and included as standard riding atoms during the least-squares refinements. Crystal data, data collection parameters, and results of the analyses are listed in Tables 1 and 2.

Compound **11** crystallized in the monoclinic crystal system. The systematic absences in the intensity data were consistent with the unique space group $P2_1/c$. The molecule lies on a center of symmetry. Only half of a formula equivalent occupies the asymmetric unit. Compound **12** crystallized in the orthorhombic crystal system. The systematic absences in the intensity data were consistent with the unique space group $P2_12_12_1$. Compound **13** crystallized in the orthorhombic crystal system. The systematic absences in the intensity data were consistent with the unique space group $C222_1$. The molecule crystallizes about a 2-fold rotation axis. Only half of a formula equivalent of the molecule is present in the asymmetric unit. One molecule of diethyl ether cocrystallized with **13** and was suitably refined with anisotropic parameters. This space group is noncentric. The Flack parameter −0.002(6) indicates that the correct enantiomorph has been selected. Compound **14** crystallized in the triclinic crystal system. The systematic absences in the intensity data were consistent with either of the space groups $P1$ or $P\bar{1}$. The latter space group was chosen and confirmed by the successful refinement of the structure. One molecule of toluene cocrystallized with **14** and was satisfactorily refined with anisotropic parameters. Compound **15** crystallized in the monoclinic crystal system. The systematic absences in the intensity data were consistent with the unique space group $P2_1/c$. A molecule of diethyl ether (refined at 25% occupancy) cocrystallized with **15**, which was disordered and modeled using geometric restraints.

Acknowledgment. This research was supported by the Office of Basic Energy Sciences of the U.S. Department of Energy under Grant DE-FG02-00ER14980.

Supporting Information Available: CIF files for each of the structural analyses. This material is available free of charge via the Internet at http://pubs.acs.org.

IC062039W

---

[23] *SAINT+*, version 6.2a; Bruker Analytical X-ray System, Inc.: Madison, WI, 2001.

[24] Sheldrick, G. M. *SHELXTL*, version 6.1; Bruker Analytical X-ray Systems, Inc.: Madison, WI, 1997.